

**Joseph R. Wasniewski**<sup>1</sup>

e-mail: joseph\_r\_wasniewski@raytheon.com

**David H. Altman**

e-mail: david\_h\_altman@raytheon.com

Raytheon Integrated Defense Systems  
Sudbury, MA 01776

**Stephen L. Hodson**

**Timothy S. Fisher**

School of Mechanical Engineering  
and Birck Nanotechnology Center,  
Purdue University,  
West Lafayette, IN 47907

**Anuradha Bulusu**

**Samuel Graham**

**Baratunde A. Cola**

George W. Woodruff School of  
Mechanical Engineering,  
Georgia Institute of Technology,  
Atlanta, GA 30318

# Characterization of Metallically Bonded Carbon Nanotube-Based Thermal Interface Materials Using a High Accuracy 1D Steady-State Technique

*The next generation of thermal interface materials (TIMs) are currently being developed to meet the increasing demands of high-powered semiconductor devices. In particular, a variety of nanostructured materials, such as carbon nanotubes (CNTs), are interesting due to their ability to provide low resistance heat transport from device-to-spreader and compliance between materials with dissimilar coefficients of thermal expansion (CTEs), but few application-ready configurations have been produced and tested. Recently, we have undertaken major efforts to develop functional nanothermal interface materials (nTIMs) based on short, vertically aligned CNTs grown on both sides of a thin interposer foil and interfaced with substrate materials via metallic bonding. A high-precision 1D steady-state test facility has been utilized to measure the performance of nTIM samples, and more importantly, to correlate performance to the controllable parameters. In this paper, we describe our material structures and the myriad permutations of parameters that have been investigated in their design. We report these nTIM thermal performance results, which include a best to-date thermal interface resistance measurement of  $3.5 \text{ mm}^2 \text{ K/W}$ , independent of applied pressure. This value is significantly better than a variety of commercially available, high-performance thermal pads and greases we tested, and compares favorably with the best results reported for CNT-based materials in an application-representative setting. [DOI: 10.1115/1.4005909]*

## 1 Introduction

As many electronic devices are moving toward higher and higher power dissipations ( $>100 \text{ W/cm}^2$ ), the need has arisen for better-performing TIMs that can greatly reduce the contact resistance to a device's heat sink or heat spreader and improve its reliability. Currently, TIMs are available commercially in a variety of different forms, including phase-change materials, greases, pastes, and epoxies, all with relatively low thermal conductivities. Without improvements in these materials, the overall temperature-drop budgets for devices may be almost completely consumed by the temperature-drop over such TIMs, making chip power density increases impractical.

Nanostructured materials such as CNTs have been studied for their use as thermal interface materials for several years, and research has corroborated their potential to provide excellent thermal transport across material boundaries [1–4]. At the heart of these materials are the nanotubes themselves, which individually offer conductivities as high as  $3000 \text{ W/m K}$  (measured) [5,6] and  $6600 \text{ W/m K}$  (predicted) [7]. When the CNTs can be aligned and oriented in the direction of heat transfer and mated to substrates, their benefits are significantly compounded [2,4,8,9]. And while such materials are interesting due to their ability to provide low resistance heat transport, they are also very attractive due to the compliance they afford between materials with dissimilar CTEs, unlike solder-based, thermal interface solutions [10,11]. Over the

last several years, different forms and configurations of interface materials have been developed utilizing CNTs, particularly vertically aligned CNTs. Nevertheless, the development of CNT-based TIMs—or nanothermal interface materials (nTIMs)—has yet to produce results which are commensurate with the high thermal conductivity found in the individual nanotubes. Some of the common processes for producing CNTs are low-pressure chemical vapor deposition (LPCVD), microwave plasma (or plasma-enhanced) chemical vapor deposition (MPCVD or PECVD), and thermal CVD. Each process has its own set of interrelated parameters that can affect the characteristics of the bulk CNT growth and translate to certain performance traits when employed in an interface material. Several reports draw some relationships between these parameters and the end effect on thermal performance [12–14], but all agree there is much left to discover and understand.

Also essential to realizing the performance advantages of nTIMs is the ability to interface them reliably with application-relevant substrate materials and test them in these configurations. Several measurement techniques have been developed to characterize nTIMs, such as the femto or nanosecond thermoreflectance [4] and photoacoustic methods [3]. While these methods can often provide valuable information regarding the thermal properties of the CNTs themselves and the interface resistances between CNTs and their growth substrates, they require samples to be configured in test structures and stackups that may not be representative of the end application. On the other hand, one-dimensional steady-state (1DSS) thermal resistance measurements provide an overall performance picture of nTIM samples as bonded to any substrates of interest based on a standard widely accepted across industry and academia. This device-to-spreader

<sup>1</sup>Corresponding author.

Contributed by the Electronic and Photonic Packaging Division of ASME for publication in the JOURNAL OF ELECTRONIC PACKAGING. Manuscript received July 12, 2011; final manuscript received November 29, 2011; published online June 11, 2012. Assoc. Editor: Dr. Madhusudan Iyengar.

(TIM1) or spreader-to-package (TIM2) thermal resistance is of ultimate importance when evaluating the nTIM in an electronics cooling application.

What follows is a description of our attempts to combine the best nTIM configurations, CNT growth conditions, and substrate-interfacing practices to arrive at interface materials that perform an order of magnitude better than current solutions, inclusive of contact resistances with interfacing substrates, as measured by a 1DSS experimental setup. We have also characterized many commercial TIMs using the precision test facility and report those results for comparison.

## 2 Approach

The following subsections describe the nTIM material, its fabrication, the thermal test facility design, and the experimental practice used to draw conclusions about the effectiveness of the material systems as thermal interfaces.

**2.1 nTIM Material Configuration.** Prior studies have shown that CNT-based materials themselves can produce thermal resistances as low as 7–8 mm<sup>2</sup> K/W (for a single CNT array between substrates) or 4 mm<sup>2</sup> K/W (two CNT arrays between mating substrates) when measured using the photoacoustic method [3,12]. In addition, a transient thermoreflectance technique used by Tong et al. [4] has measured a thermal resistance of 12 mm<sup>2</sup> K/W imparted by a Si-CNT-glass interface. However, one persistent challenge facing nTIMs has been overcoming the high contribution (as much as 90%) of nTIM-to-substrate thermal resistance to the overall thermal resistance when the device and spreader/sink are mated [2–4,10,11,15,16]. Engaging a high percentage of the free CNT tips in the array is one major part of this problem. However, some recently contrived configurations of nTIMs make use of a thin, compliant, metallic interposer foil, on which CNTs are grown on both sides [15,17]. The compliant foil, along with axially compliant CNT arrays, has presumably served to increase free tip engagement, especially when moderate pressure is applied to the material stack. Furthermore, this CNT configuration now makes for a drop-in solution between many types of substrates, as direct-growth (at high temperature) onto the substrate is not required. Cola et al. [15] found the resistance of this type of double-sided CNT stackup to be 10 mm<sup>2</sup> K/W via photoacoustic analysis. The nTIM stackups utilized in our experiments mimic this double-sided, multiwalled CNT (MWCNT) structure, as is shown in Fig 1.

**2.2 CNT Growth and nTIM Fabrication.** Starting with a 10 μm copper or aluminum foil, CNTs are grown simultaneously on both sides using either an LPCVD or MPCVD process, by Georgia Institute of Technology and Purdue University, respectively. To perform MPCVD growth on copper foil, a trilayer catalyst film of Ti 30–60/Al 10/Fe 3–4 nm is evaporated onto the foil. Similarly, a catalyst stack of Ti 20–60/Al 10/Fe 3–5 nm or Ni 100/Ti 30/Al 10/Fe 3 nm was used to make all the LPCVD samples on aluminum foils. MPCVD samples were grown using 20% CH<sub>4</sub> in H<sub>2</sub> at 10 Torr and 800 °C, unless otherwise noted. The LPCVD recipe utilized 5% C<sub>2</sub>H<sub>2</sub> in H<sub>2</sub> at 7.5 Torr and 650 °C, followed by annealing in N<sub>2</sub> for 5 min at a temperature of 500 °C, for most experiments.

The synthesis parameters varied to achieve different CNT growths and morphologies include substrate temperature and growth time for LPCVD and substrate temperature, plasma power, and DC bias for MPCVD. Prior studies, especially for those using PECVD and MPCVD [1,12,14] had already attempted to correlate these different “recipes” to CNT properties affecting their thermal resistance in bulk: variation in heights, densities, tube diameters, and stiffnesses of the CNTs. Therefore, many aspects of these “best recipes” were utilized as a starting point for our investigation of the optimal processing parameters.

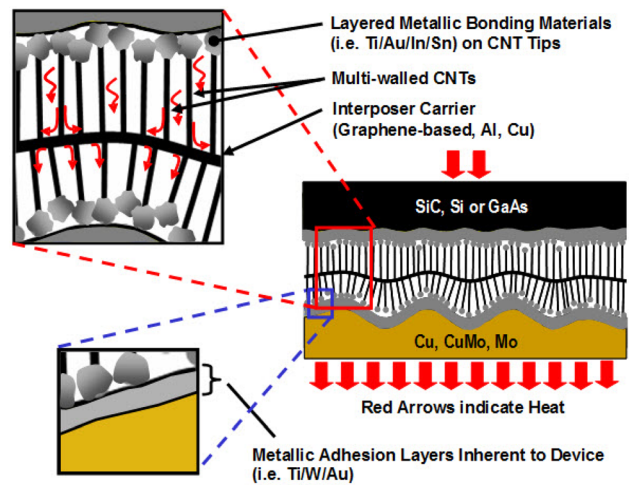


**Fig. 1** The basic structure of our nTIM consists of MWCNTs grown on both sides of an interposer foil and interfaced with various substrates via a metallic bond

**2.3 Metallic Bonding Techniques.** In order to address CNT free tip engagement—and to provide a structural bond between the nTIM and the substrate(s)—two metallic bonding techniques were explored in parallel. The first was the use of palladium nanoparticles as a thermally conductive bonding mechanism. Hodson et al. [18] had demonstrated thermal resistances of 5 mm<sup>2</sup> K/W via photoacoustic measurement using palladium hexadecanethiolate applied to both interfaces of a double-sided nTIM. The preparation, application, and processing of this solution as a bonding agent is described in detail in that work. The second method investigated for bonding nTIMs to substrates was thermocompression to promote diffusion between the substrate and the nTIM, similar to the process described in Ref. [19]. In this technique, the free tips of the CNTs are coated (via electron beam evaporation) with gold metalization stackups (typically Ti 60/Au 250 nm) then mated to substrates with similarly coated metalization stackups (typically Ni 100/Au 500 nm) to form a gold–gold diffusion bond under the application of low temperature (<240 °C) and mild pressure (<30 psi). As a tangent activity to the experimentation performed with diffusion bonding, we also attempted to bond nTIM samples to CuMo and SiC substrates using solder foils of various compositions, as will be discussed. Since surface roughness of the substrates to be mated to the nTIMs is assumed to be important to attaining high free tip engagement and uniform bonding, each CuMo test substrate (described below) was ground to achieve no greater than 0.75 μm average roughness (typically less than 0.50 μm), which is significantly rougher than one would expect for a heat spreader or package surface. The SiC substrates utilized possessed a mirror finish as typical of wafer processing.

**2.4 Characterization Test Facility.** Because carbon nanotube-based thermal interface materials have the potential to provide thermal resistances an order of magnitude lower than current commercially available solutions, their characterization requires an innovative testing approach, with precision similar to those approaches utilized by others measuring very low resistance materials [20,21]. Our solution involved the design of a test facility tailored to the characterization of these new nTIMs, allowing the accurate measurement of thermal resistances down to 4 mm<sup>2</sup> K/W or better and capturing the interface physics resulting from CTE-mismatched semiconductors and packaging materials. This facility is based on the widely used ASTM D 5470 approach [22] but incorporates several enhancements. It provides the capability of testing extremely thin TIMs (on the order of 25 μm thickness) as well as a variety of alternative interface materials (gaskets, pastes, greases) at a range of contact pressures. The facility also

forsakes idealized test surfaces in favor of true device-to-spreader application conditions by interfacing the nTIM with silicon carbide and/or copper-molybdenum.

The nTIM test facility (Fig. 2) has been designed to allow the testing of a single sample or a “stack” of samples, whereby SiC is sandwiched between two nTIMs. The single sample or sample stack is placed between two 1 cm<sup>2</sup>, 38-cm long reference bars, or meter bars, of copper-molybdenum composite material (15/85 composition) possessing a CTE of approximately 7 ppm/°C. The meter bars are precisely aligned in the test facility, where the sample(s) can undergo testing in a “dry” (unbonded) configuration or be bonded in situ to the bars prior to testing. A precision linear guide is used to achieve meter bar alignment and low-friction sliding under thermal expansion, while ball-in-socket joints at both ends of the test subassembly absorb any residual misalignment and bar surface nonplanarity. Insulating thermoplastic components were designed to enable minimal heat loss (less than 10%), and high-precision thermistors were calibrated for very accurate temperature measurements (to within 0.03 °C). Bonding and material testing pressures of up to 100 psi can be applied and measured via a compression spring and load cell, respectively. A thorough but conservative uncertainty analysis similar to Ref. [21] using the Brown, Coleman, and Steele methodology [23] predicts a measurement uncertainty of 15% or lower for thermal resistances as low as 4 mm<sup>2</sup> K/W. The main drivers of experimental uncertainty are thermistor hole location measurements along the length of the meter bars and float of the thermistors in their holes due to diametric clearance.

**2.5 Experimental Approach.** Over the course of 10 months, the 1DSS thermal test facility was utilized to perform nearly 200 tests of various nTIM samples and 25 tests of commercially available thermal interface materials. Initially, tests were performed on nTIMs derived from best-known CNT growth recipes and processing parameters but bonded to our CuMo substrates using the palladium thiolate and gold diffusion bonding approaches. The typical flow for testing an nTIM sample or sample stack consisted of the following:

- Assembly of the sample(s) between the CuMo meter bars (the bars already interfaced with a coldplate on one side and a copper heater block with an embedded cartridge heater on the other side)

- Bonding (if desired) under the chosen pressure and temperature conditions
- Thermal resistance testing at approximately 20, 40, and 60 psi
- Post-test destructive analysis (qualitative bond strength determination and fracture analysis)
- –(or)–
- Cycling and stability testing, followed by another thermal interface resistance test, then destruction
- Resurfacing of the meter bars to a designated roughness
- Remetalization of the meter bar surfaces (if desired)

Testing largely followed a systematic approach to investigate the effects of the many sample variables on overall thermal performance. Regarding CNT growth, these tests included varying growth parameters for the LPCVD and MPCVD processes (time/temperature and time/plasma power/DC bias, respectively). The choice of interposer metal and its thickness was also studied, but we found no conclusive effect on performance. There were also many variables within the bonding processes to be explored. For palladium thiolate bonding, these included various solution compositions, solution volumes applied, and thermolysis temperatures and pressures (refer to Ref. [18]); for diffusion bonding, several metalization stackups and thicknesses were evaluated, while altering bond pressures and temperatures.

The tests performed often provided insights regarding the main contributors to performance, which were in-turn examined more closely. Subsequent to processing parameter vetting and optimization, the testing focus then turned to several enhancement techniques we hoped would push our nTIMs closer to achieving the desired thermal resistance numbers. For instance, single sample tests interfacing CuMo on both sides were compared against sample “stack” tests, using samples grown within the same batch, to understand if the inclusion of a polished and metalized SiC tab played a role in CNT surface compliance and thermal performance. Additionally, postgrowth microwave annealing of CNTs was evaluated against the same nonannealed CNT samples. Our team also pursued the use of wicked-in fillers such as paraffin wax that could potentially improve thermal transport. Lastly, the use of solder at the nTIM-to-substrate bond interfaces was aggressively pursued as a more repeatable alternative to gold diffusion bonding. These enhancement techniques provided some of the most

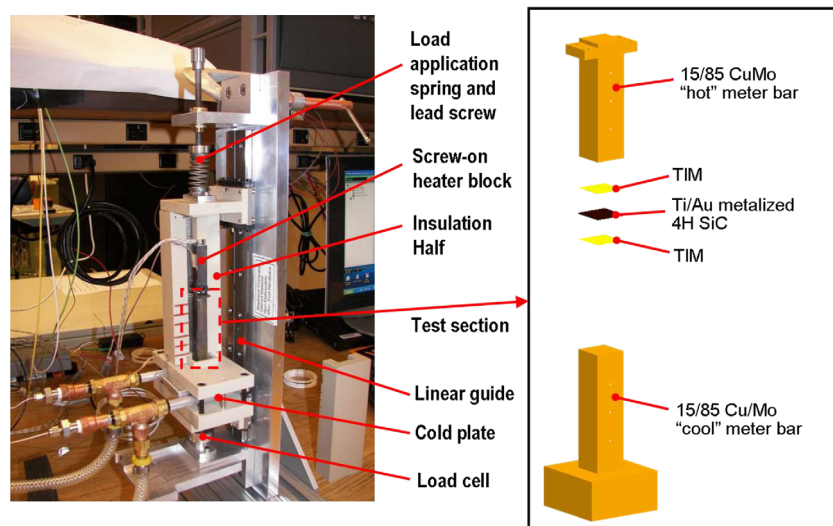


Fig. 2 The 1D steady-state test facility derived from ASTM D 5470 can test a variety of materials in different configurations. A sample “stack” test setup is shown on the right.

distinct differences in thermal resistance test results and are emphasized as such below.

### 3 Results

A report on the outcome of all the experiments involving the different parameter combinations and variations tested would be much too lengthy for inclusion here, but the most technologically relevant results and conclusions are discussed below.

#### 3.1 nano-TIM Testing

**3.1.1 Palladium Thiolate Versus Gold Diffusion Bonding.** One major observation throughout our testing regarded the effectiveness of each type of metallic bonding attempted. Subsequent to many trials, it became very clear that palladium thiolate bonding of the nTIM samples was enabling lower levels of overall thermal resistance. Sometimes the effect (comparing a test without palladium thiolate to one with palladium thiolate) was substantial. For example, whereas the lowest thermal resistance for a dry-interface MPCVD sample was 41 mm<sup>2</sup> K/W (200 W power, 100 V bias, 2.5 min CNT growth conditions), the lowest for a palladium-bonded sample was 25 mm<sup>2</sup> K/W (100 W power, 0 V bias, 2.5 min growth), as shown in Fig. 3. The heights of the CNTs measured on each side of the interposer (copper) foil for these samples were 4–7 μm and 1–3 μm, respectively, which are shorter than most other nTIM samples tested but were later found to have little impact on thermal resistance compared to samples with taller CNTs discussed elsewhere in this paper. The average surface roughness of the CuMo meter bars they were interfaced with was 0.48 and 0.50 μm. We note that these resistance results are generally consistent with expectations because an interposer foil with CNTs on each side contains twice the number of heterogeneous material interfaces as previously reported for dry, “single-sided” CNT interfaces that produce roughly half of the present resistance values [3]. Furthermore, besides adding mechanical robustness to each interface (CNT to CuMo and/or CNT to SiC), the palladium-bonded nTIMs sustained uniformly lower resistances independent of pressure exerted on the interface (i.e., the resistance values are maintained down to no-load conditions). This is of course a very significant benefit for certain applications, such as die-attach. A common trait among the aforementioned results, and validated by other experiments, is the lower overall thermal resistance that shorter CNT growth times (2.5 and 5 min) generated for the MPCVD and LPCVD processes when tested in both unbonded and bonded configurations.

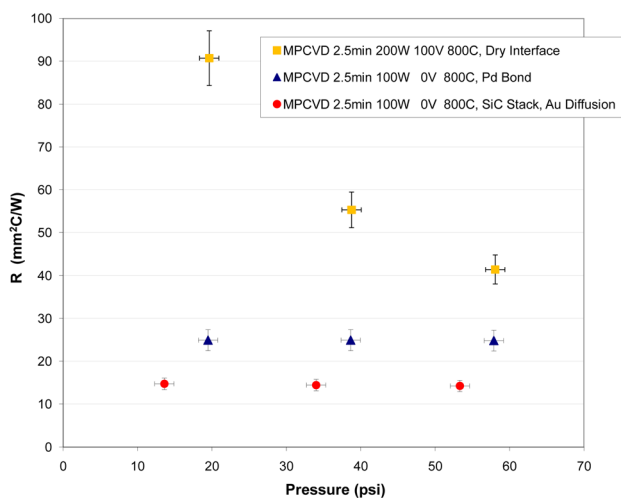


**Fig. 3 Best 1DSS test results for MPCVD-produced nTIM samples tested bare (dry), with Pd thiolate, and using Au diffusion**

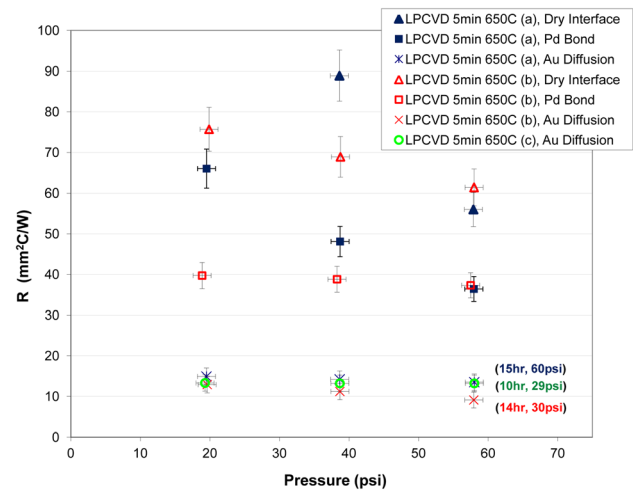


**Fig. 4 Best 1DSS test results for LPCVD-produced nTIM samples tested bare (dry), with Pd thiolate, and using Au diffusion**

Tests utilizing diffusion bonding with LPCVD-produced nTIMs yielded some of the best overall results. Two sample batches created under the same conditions of 5-min, 650°C growth were responsible for very good thermal resistances, as depicted in Fig. 4. Even under the same growth conditions, average CNTs heights on each side of the aluminum foil were measured to be 7–13 μm for one batch (a) and 9–12 μm for the other (b). Samples tested from these batches using dry interfaces did not have metalized CNT tips and were interfaced with meter bars surfaces of 0.36–0.46 μm average roughness. For both sample batches, the use of palladium thiolate (2 h, 30 psi processing) clearly provided a performance advantage over the same nTIMs tested in an unbonded configuration. Gold diffusion bonding offered an even more substantial thermal resistance improvement—down to 14 mm<sup>2</sup> K/W and 9 mm<sup>2</sup> K/W. However, these results proved very difficult to replicate; challenges with achieving strong, uniform diffusion bonds, and instances of delamination of the CNTs from the interposer foil precluded positive test results. Furthermore, gold diffusion bonding of the two samples were performed under differing conditions: for 15 h at 60 psi pressure and for 14 h at 30 psi pressure, as noted in Fig. 4. There was concern that the low thermal resistances we had measured for these samples were attributable mostly to the long-duration and/or high-pressure bonding conditions, and that similar results might not be achievable under stricter (< 10 h, < 30 psi) processing limits. Nevertheless, subsequent tests for bonded samples processed at 10 h and 30 psi yielded resistances in the sub-30 mm<sup>2</sup> K/W range. This includes the thermal resistance result of 13 mm<sup>2</sup> K/W achieved for a third LPCVD batch (c) produced under the same conditions as (a) and (b), with CNT heights averaging 9–12 μm, interfaced to CuMo bars with roughnesses of 0.36 and 0.45 μm.

Gold diffusion bonding was also attempted using a sample “stack” configuration—nTIM-SiC-nTIM—between the CuMo meter bars to investigate the impact, both mechanical and thermal, that substrate material (and typical corresponding surface roughness) might have on the diffusion bonding process and the overall resistance through the two nTIM samples; the polished and metalized surface of the SiC tab offers a different contact interface as well as phonon interface with the metalized CNT tips. Most samples bonded in this stackup resulted in more uniform bonding, as indicated by our post-test destructive assessments. Still, resistance measurements over a broad range of tests did not indicate any consistent improvement in performance.

**3.1.2 Effect of Microwave Annealing.** Several other nTIM enhancement techniques were pursued in an attempt to decrease thermal resistance. For example, we explored microwave annealing

of the nTIMs after CNT growth as a means of more strongly anchoring the CNTs to the interposer foil via the catalyst layer. A study by Lin et al. [24] had shown a distinct reduction in the defects found in the CNTs when examined by Raman spectroscopy and X-ray photoelectron spectroscopy. Therefore, we attempted a similar postgrowth microwave annealing at 2.45 GHz, at a power level of 1300 W, and with exposure times of 5, 10, and 15 min. The samples were tested in a “stack” configuration using a metalized SiC tab (Ti 60/Au 250 nm) between two identical nTIM samples. In our tests with these annealed samples, we found that no particular microwave exposure time provided a clear benefit over any of the others, but nTIMs annealed with microwave radiation did consistently out-perform nTIMs that were left untreated—even though the performance benefit varied. Furthermore, through qualitative analysis, we found that microwave annealing provided stronger bonds between the CNTs and their interposer foil (whereas other samples would often easily delaminate from the foil when bonded in a “stack” configuration). We suspect this is related to the reduced CNT defect density that microwave annealing seems to impart.

**3.1.3 Effect of Wax Infiltration.** Cola et al. [9] demonstrated that the addition of paraffin wax (wicked in liquid state into the CNT arrays from the edges) served to reduce the bulk thermal resistance of a CNT-based interface material placed between two substrates (Si and Ag). The researchers postulated that the wax served to provide an improved thermal path (rather than air) between free (unbonded) CNT tips and the mating substrate. A reduction of more than 50% in thermal resistance was measured after the addition of the wax to various CNT arrays. Figure 5 details the effectiveness of wax infiltration in improving the thermal resistance of our own nTIMs. Samples produced by LPCVD (5 min, 650 °C growth on aluminum foil), which were subsequently microwave-annealed, were interfaced to SiC on one side and CuMo (0.31 and 0.46  $\mu\text{m}$  roughnesses) on the other side in a stack configuration via gold diffusion bonding for 10 h at 26 psi. When wax was added at the conclusion of the initial diffusion bonding procedure, at least a 30% reduction in thermal resistance was realized for each sample. Some of our best results were obtained when using wax infiltration with this particular LPCVD batch: as low as 10.4  $\text{mm}^2 \text{K/W}$ . We are currently investigating the effects of other varieties of wax as well as other filler agents for improved nTIM performance.

Samples infiltrated with wax following diffusion bonding were also subjected to thermal cycling and stability tests to determine how the interfaces held up under application temperature extremes

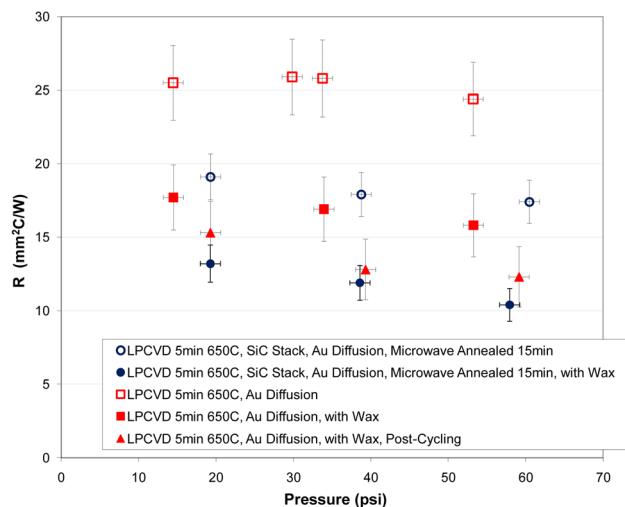


**Fig. 5 A comparison of test results for LPCVD-grown nTIMs before and after infiltration of the CNT arrays with wax. One wax-infiltrated sample was also thermally cycled and retested to check for sustained performance.**

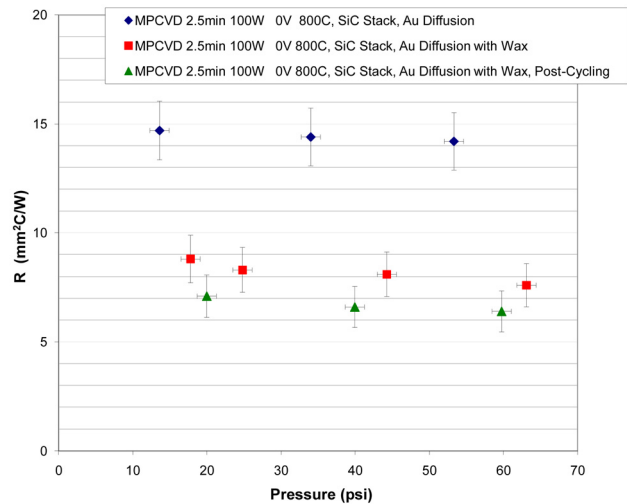


**Fig. 6 Results for MPCVD-grown samples tested in a stack just after diffusion bonding, after the further addition of wax, and after cycling of the wax-infiltrated bonds**

(cycling from 0 °C to 70 °C for 10 cycles and stable at 130 °C for 100 h). We found that for multiple tests, such as those of the LPCVD (5 min, 650 °C) batch depicted in Fig. 5 and the MPCVD (100 W power, 0 V bias, 800 °C, 2.5 min) samples of Fig. 6, the thermal resistance of the wax-treated nTIMs actually improved when retested upon the completion of thermal cycling. This is likely attributable to the additional time allowed for the wax to further permeate the CNT arrays. After the addition of wax, and postcycling, the average interface resistances for the MPCVD samples shown were very low: 7.6 and 6.4  $\text{mm}^2 \text{K/W}$ , respectively. Initial diffusion bonding of these cycled LPCVD and MPCVD samples occurred for 10 h at 30 psi to SiC and/or CuMo bar surfaces (0.21–0.35  $\mu\text{m}$  roughnesses) as noted by the figure legends.

**3.1.4 Effect of Gold Thickness for Diffusion Bonding.** After limited success using gold diffusion bonding, experiments were conducted to investigate the role of evaporated gold thickness onto the CNT arrays on their effective resistances. It was thought that different metalization thicknesses might affect the ability of the CNTs to comply to substrate surfaces of different microscale and nanoscale geometries, and thus firmly contact and bond to a metalized substrate. The buildup of the gold on the CNTs would obviously determine if the gold formed a cohesive surface layer over the CNTs or globules on the free tips that preserved the individual motion of each CNT, and this difference could affect the deformation mechanics. Three thicknesses of gold deposition (150, 250, and 350 nm) over 60 nm titanium were compared using CNTs grown from the exact same batch and thus possessing identical growth and processing conditions. The results (see Fig. 7) indicated that the metalization thicknesses, when varied in this range, do not appear to consistently correlate to better or worse thermal performance (or a noticeable difference in the quality of the bond to the substrate). Figure 7 also compares annealed (1300 W, 5 min exposure) to nonannealed samples of the same CNT growth properties and metalization. The improvement that the annealing provides is apparent, consistent with conclusions discussed earlier.

**3.1.5 Solder Bonding of nTIMs.** Most recently, 1DSS tests have been performed using a different approach to metallic bonding: solder foil bonding. Thin (0.051 mm thick) foils of several low-melting point solder alloys were used as a substitute for diffusion bonding, whereby the solder foil is placed between the CNT free tip surfaces and the substrate, brought above its eutectic point, and then cooled to form a solid filler between the two. This

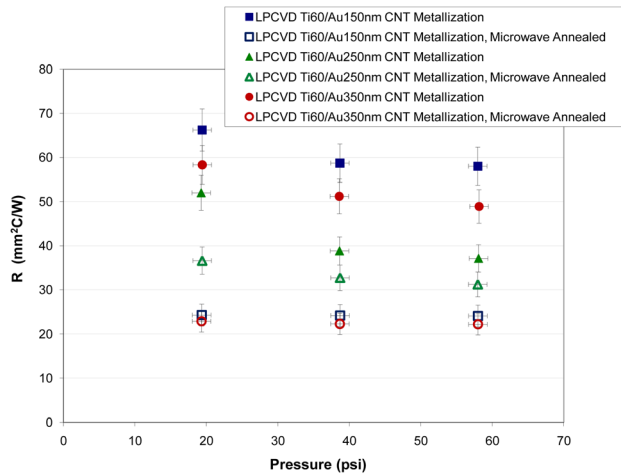


Fig. 7 LPCVD nTIM samples of varying gold metalization thicknesses (over CNT tips), with and without microwave annealing

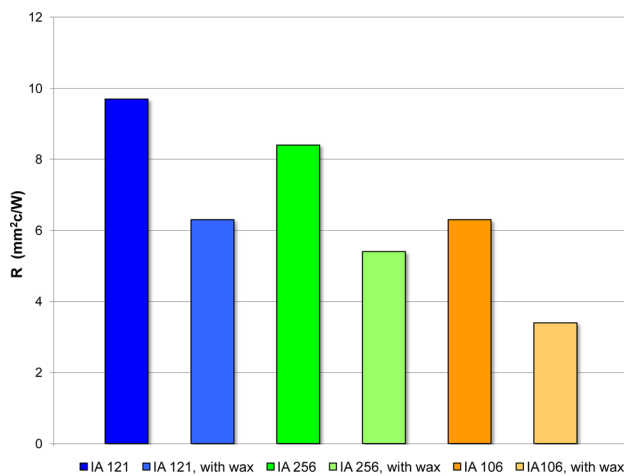


Fig. 8 MPCVD samples interfaced to CuMo meter bar substrates via solder foil bonds of various compositions, with and without wax

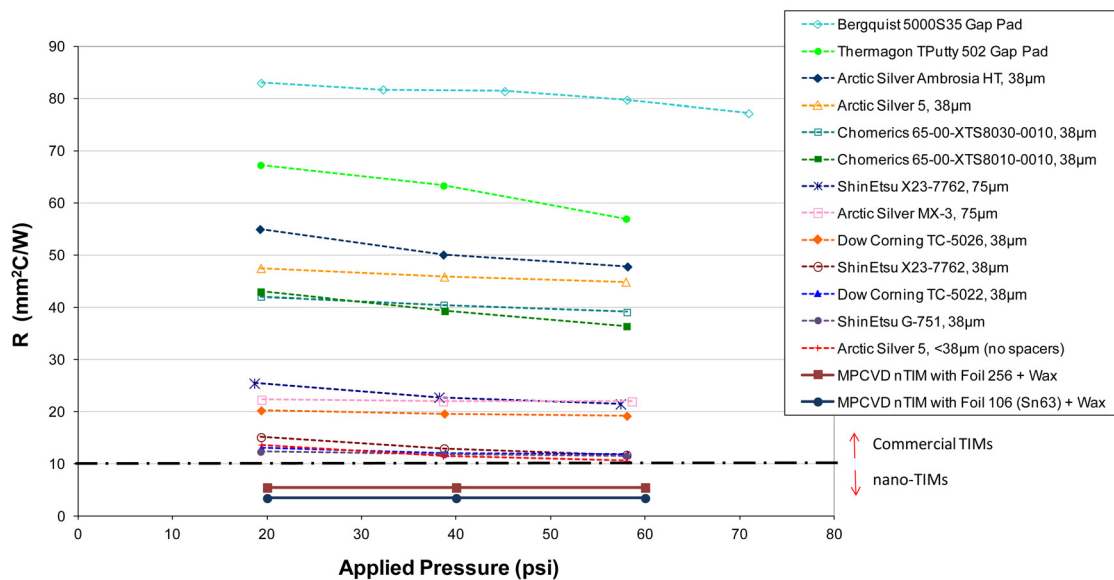


Fig. 9 A summary of commercial thermal interface materials tested in the 1DSS facility, with a comparison to nTIMs

approach has been attempted previously using CNTs, particularly with indium, as reported in prior literature [4,16]. The motivation for using solder foils was to produce more repeatable results in terms of bond strength and thermal performance, since the ability of the solder to flow could compensate for surface roughness conditions, surface asperities, etc., that make diffusion bonding very difficult. The sole use of low-melting point solders and indium foils as interface materials, and of reacting foils such as Indium Corporation's NanoFoil<sup>®</sup> in conjunction with higher flow temperature solders, still depends on highly planar, wettable bonding surfaces and offers too high a modulus to compensate for CTE mismatch. Thus, the nTIM is essential, and several different solder compositions were tested having liquidus temperatures in a suitable range for device operating (low end) and rework (high end) conditions:

- Indalloy<sup>®</sup> 121, Sn96.5% Ag3.5%, 221 °C
- Indalloy<sup>®</sup> 256, Sn96.5% Ag3.0% Cu0.5%, 220 °C
- Indalloy<sup>®</sup> 106, Sn63.0% Pb37.0%, 183 °C

The solder foil approach was utilized with various bonding temperatures 10–30 °C above each foil's liquidus temperature for 30 s, all at 30 psi applied interface pressure. Overall, the solder foil tests were very successful in providing strong bonds and low interface resistances. Figure 8 showcases representative results for solder foil bonding with samples grown by MPCVD (100 W power, 0 V bias, 800 °C, 2.5-min CNT growth). As is evident by these results and others, the Indalloy<sup>®</sup> 106 (Sn63%/Pb37%) samples outperformed the samples bonded using the Indalloy<sup>®</sup> 256 and 121 solder foils. In fact, the MPCVD samples bonded with the Sn63/Pb37 foils consistently achieved resistances similar to those shown here of 6.3 mm<sup>2</sup> K/W and 3.4 mm<sup>2</sup> K/W (with the addition of wax). Once again, we see that wax does serve to further decrease the thermal resistance of each bonded sample.

**3.2 Commercial TIM Testing.** While testing the nanothermal interface materials discussed in this paper, we also found it worthwhile to characterize several commercially available thermal interface materials (greases, pastes, and pads only), particularly those commonly used and/or purported by literature to possess the highest conductivities. Most commercially available TIMs advertise thermal conductivities in the range of 1–10 W/m K, which when applied as thin uniform layers can achieve thermal interfaces resistances comparable to those of the nTIMs discussed here.

For these tests, the 1DSS test facility was utilized, but with oxygen-free copper meter bars rather than copper-molybdenum bars, having the same surface roughness. The use of pure copper is inconsequential but results in slightly less measurement uncertainty due to its precisely known and higher value of thermal conductivity, which allows for a wider temperature gradient through the bars and interface material. Identical test procedures were followed, and data points for each sample were taken in the same range of applied pressure as the nTIM tests. The only differences were that no permanent bonding to the substrates took place (since the commercial materials used were removable) and the greases were mixed with spacer beads (38  $\mu\text{m}$  or 75  $\mu\text{m}$  diameter) 2–5% by weight to achieve known interface thicknesses in the typical thickness range of an nTIM.

The outcome of these tests is summarized in Fig. 9, with the legend listing the materials in order of average thermal resistance measured (highest to lowest from top to bottom). Except where noted as gap pads, these materials were mainly thermal greases. They exhibited a wide range of thermal resistance values, some more pressure-dependent than others, with the lowest resistances being achieved by Shin-Etsu<sup>®</sup> G-751, Shin-Etsu<sup>®</sup> X23-7762, and Dow Corning<sup>®</sup> TC-5022—all measuring about 10  $\text{mm}^2$  K/W when controlled to a 38  $\mu\text{m}$  thickness. Also evident is that the nTIMs developed as part of this effort and through many of the research efforts referenced in this paper out-perform many high-performing commercial materials by several fold.

#### 4 Conclusions

We have developed a one-dimensional steady-state test facility capable of accurately measuring thermal interface resistances of state-of-the-art interface materials under device-to-spreader application conditions. We have also successfully attempted to stitch together promising pieces of research completed in the last several years to derive an optimal nanothermal interface material capable of meeting the thermal requirements of the next generation of high-powered electronic devices. The incorporation of extremely conductive carbon nanotubes with compliant yet strong metallic interposer foils results in an nTIM that is easily interfaced with a variety of substrates for different applications, is mechanically robust and compliant to CTE mismatch, and can provide a high-conductivity thermal path from an electronic device to a heat sink. We have incorporated several enhancements to this material, including wax infiltration and microwave annealing of CNTs, that each provides incremental decreases in thermal resistance. Still, there is much work to be done to optimize the carbon nanotube characteristics and substrate-interfacing techniques to realize the full potential of such CNT-based materials. Nevertheless, the materials described herein have demonstrated interface resistances significantly better than all commercial materials we tested and compare favorably with the best steady-state results reported for CNT-based nTIMs in an application-representative setting.

#### Acknowledgment

We are very grateful for the important contributions of Olalekan S. Adewuyi to CNT growth on aluminum foil using LPCVD as well as Parisa Pour Shahid Saeed Abadi and John H. Taphouse for experimental support (CNT growth and metalization) at Georgia Institute of Technology. Thanks also to Anurag Gupta of Raytheon Integrated Defense systems for his design and analysis support and to Story Wibby for his experimental support and data processing. In addition, the authors would like to gratefully acknowledge Dr. Thomas Kenny for his leadership of the Nano-Thermal Interfaces (NTI) Program of the Defense Advanced Research Projects Agency (DARPA). This material is based upon work supported by DARPA and the Space and Naval Warfare (SPAWAR) Systems Center, Pacific under Contract No. N66001-09-C-2013. The views expressed are those of the author and do

not reflect the official policy or position of the Department of Defense or the U.S. Government. Distribution Statement A (Approved for Public Release, Distribution Unlimited), Case Number 16885, February 15, 2011.

#### References

- [1] Xu, J., and Fisher, T. S., 2006, "Enhanced Thermal Contact Conductance Using Carbon Nanotube Array Interfaces," *IEEE Trans. Compon., Packag. Technol.*, **29**(2), pp. 261–267.
- [2] Hu, X. J., Padilla, A. A., Xu, J., Fisher, T. S., and Goodson, K. E., 2006, "3-Omega Measurements of Vertically Oriented Carbon Nanotubes on Silicon," *ASME J. Heat Transfer*, **128**, pp. 1109–1113.
- [3] Cola, B. A., Xu, J., Cheng, C., Xu, X., Fisher, T. S., and Hu, H., 2007, "Photoacoustic Characterization of Carbon Nanotube Array Thermal Interfaces," *J. Appl. Phys.*, **101**, p. 054313.
- [4] Tong, T., Zhao, Y., Delzeit, L., Kashani, A., Meyyappan, M., and Majumdar, A., 2007, "Dense Vertically Aligned Multiwalled Carbon Nanotube Arrays as Thermal Interface Materials," *IEEE Trans. Compon., Packag. Technol.*, **30**(1), pp. 92–100.
- [5] Kim, P., Shi, L., Majumdar, A., and McEuen, P. L., 2001, "Thermal Transport Measurements of Individual Multiwalled Nanotubes," *Phys. Rev. Lett.*, **87**(21), p. 215502.
- [6] Yu, C., Shi, L., Yao, Z., Li, D., and Majumdar, A., 2005, "Thermal Conductance and Thermopower of an Individual Single-Wall Carbon Nanotube," *Nano Lett.*, **5**(9), pp. 1842–1846.
- [7] Berber, S., Kwon, Y.-K., and Tomanek, D., 2000, "Unusually High Thermal Conductivity of Carbon Nanotubes," *Phys. Rev. Lett.*, **84**(20), pp. 4613–4616.
- [8] Wang, H., Feng, J. Y., Hu, X. J., and Ng, K. M., 2010, "Reducing Thermal Contact Resistance Using a Bilayer Aligned CNT Thermal Interface Material," *Chem. Eng. Sci.*, **65**, pp. 1101–1108.
- [9] Cola, B. A., Hodson, S. L., Xu, X., and Fisher, T. S., 2008, "Carbon Nanotube Array Thermal Interfaces Enhanced With Paraffin Wax," Proceedings of the ASME Summer Heat Transfer Conference, Paper No. HT2008-56483.
- [10] Zhang, Y., Xu, Y., Suhir, E., Gu, C., and Lui, X., 2008, "Compliance Properties Study of Carbon Nanofibers (CNFs) Array as Thermal Interface Material," *J. Phys. D: Appl. Phys.*, **41**, p. 155105.
- [11] Cola, B. A., Xu, J., and Fisher, T. S., 2009, "Contact Mechanics and Thermal Conductance of Carbon Nanotube Array Interfaces," *Int. J. Heat Mass Transfer*, **52**, pp. 3490–3503.
- [12] Cola, B. A., Amama, P. B., Xu, X., and Fisher, T. S., 2008, "Effects of Growth Temperature on Carbon Nanotube Array Thermal Interfaces," *ASME J. Heat Transfer*, **130**, p. 114503.
- [13] Liu, X., Zhang, Y., Cassell, A. M., and Cruden, B. A., 2008, "Implications of Catalyst Control for Carbon Nanotube Based Thermal Interface Materials," *J. Appl. Phys.*, **104**, p. 084310.
- [14] Maschmann, M. R., Amama, P. B., Goyal, A., Iqbal, Z., and Gat, R., 2006, "Parametric Study of Synthesis Conditions in Plasma-Enhanced CVD of High-Quality Single-Walled Carbon Nanotubes," *Carbon*, **44**, pp. 10–18.
- [15] Cola, B. A., Xu, X., and Fisher, T. S., 2007, "Increased Real Contact in Thermal Interfaces: A Carbon Nanotube/Foil Material," *Appl. Phys. Lett.*, **90**, p. 093513.
- [16] Tong, T., Zhao, Y., and Delzeit, L., 2006, "Indium Assisted Multiwalled Carbon Nanotube Array Thermal Interface Materials," *Proceedings of the Intersociety Conference on Thermal and Thermomechanical Phenomena in Electronic Systems (ITHERM)*, pp. 1406–1411.
- [17] Wang, H., Feng, J., Hu, X., and Ng, K. M., 2007, "Synthesis of Aligned Carbon Nanotubes on Double-Sided Metallic Substrate by Chemical Vapor Deposition," *J. Phys. Chem. C*, **111**, pp. 12617–12624.
- [18] Hodson, S. L., Bhuvana, T., Cola, B. A., Xu, X., Kulkarni, G. U., and Fisher, T. S., 2011, "Palladium Thiolate Bonding of Carbon Nanotube Thermal Interfaces," *ASME J. Electron. Packag.*, **133**, p. 020907.
- [19] Johnson, R. D., Bahr, D. F., Richards, C. D., Richards, R. F., McClain, D., Green, J., and Jiao, J., 2009, "Thermocompression Bonding of Vertically Aligned Carbon Nanotube Turfs to Metalized Substrates," *Nanotechnology*, **20**, p. 065703.
- [20] Kearns, D., 2003, "Improving Accuracy and Flexibility of ASTM D 5470 for High Performance Thermal Interface Materials," *Proceedings of 19th IEEE Semiconductor Thermal Measurement and Management Symposium (SEMI-THERM)*, pp. 129–133.
- [21] Kempers, R., Kolodner, P., Lyons, A., and Robinson, A. J., 2008, "Development of a High-Accuracy Thermal Interface Material Tester," *Proceedings of the Intersociety Conference on Thermal and Thermomechanical Phenomena in Electronic Systems (ITHERM)*, pp. 221–226.
- [22] ASTM, 2006, *Standard Test Methods for Thermal Transmission Properties of Thin Thermally Conductive Solid Electrical Insulation Materials*, Conshohocken, PA.
- [23] Brown, K. K., Coleman, H. W., and Steele, W. G., 1995, "Estimating Uncertainty Intervals for Linear Regression," *Proceedings of the 33rd American Institute of Aeronautics and Astronautics Aerospace Sciences Meeting and Exhibit*, pp. 9–12.
- [24] Lin, W., Moon, K.-S., Zhang, S., Ding, Y., Shang, J., Chen, M., and Wong, C.-P., 2010, "Microwave Makes Carbon Nanotubes Less Defective," *ACS Nano*, **4**(3), pp. 1716–1722.